

Accepted Manuscript

A benzothiazole-based fluorescent probe for selective detection of H₂S in living cells and mouse hippocampal tissues

Yi Liu, Yan Ding, Jie Huang, Xiaofei Zhang, Tongyong Fang, Yuyun Zhang, Xian Zheng, Xia Yang

PII: S0143-7208(16)30712-4

DOI: [10.1016/j.dyepig.2016.11.038](https://doi.org/10.1016/j.dyepig.2016.11.038)

Reference: DYPI 5607

To appear in: *Dyes and Pigments*

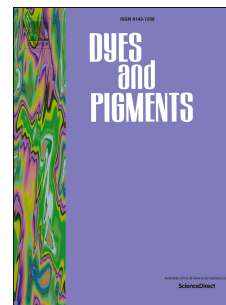
Received Date: 13 September 2016

Revised Date: 22 October 2016

Accepted Date: 20 November 2016

Please cite this article as: Liu Y, Ding Y, Huang J, Zhang X, Fang T, Zhang Y, Zheng X, Yang X, A benzothiazole-based fluorescent probe for selective detection of H₂S in living cells and mouse hippocampal tissues, *Dyes and Pigments* (2016), doi: [10.1016/j.dyepig.2016.11.038](https://doi.org/10.1016/j.dyepig.2016.11.038).

This is a PDF file of an unedited manuscript that has been accepted for publication. As a service to our customers we are providing this early version of the manuscript. The manuscript will undergo copyediting, typesetting, and review of the resulting proof before it is published in its final form. Please note that during the production process errors may be discovered which could affect the content, and all legal disclaimers that apply to the journal pertain.



1 **A benzothiazole-based fluorescent probe for selective detection of H₂S**
2 **in living cells and mouse hippocampal tissues**

3
4 Yi Liu,^{#*a} Yan Ding,^{*a} Jie Huang,^a Xiaofei Zhang,^a Tongyong Fang,^a Yuyun Zhang,^a
5 Xian Zheng,^a and Xia Yang^a

6
7 ^a Jiangsu Key Laboratory of New Drug Research and Clinical Pharmacy, School of
8 Pharmacy, Xuzhou Medical University, Xuzhou, Jiangsu 221004, China.

9
10 [#] Fax: +86-0516-83262136, E-mail: cbpeluyinew@163.com.

11
12 †Electronic Supplementary Information (ESI) available: Synthesis, additional
13 methods, additional plots of UV and fluorescence, NMR and HR-MS analysis data,
14 additional other supporting data.

15
16 *These authors contributed equally to this paper.

17 **Abstract**

18 This study reports a benzothiazole-based fluorescent probe EPS-HS for real-time
19 detection of H₂S. The probe is characterized in a large red-shift, good selectivity, high
20 sensitivity and favorable biocompatibility. We measured the detection limit of
21 EPS-HS in PBS buffer and fetal bovine serum. Moreover, in HT22 living cell imaging
22 studies, EPS-HS showed good cell permeability and H₂S could be detected within the
23 cells. Furthermore, *in situ* visualization of H₂S was performed on the hippocampal
24 slices of normal mice with EPS-HS. We were also able to estimate the concentration
25 of sulfide in mouse hippocampus tissues. The probe will be applied for better
26 treatment of neurological deficits caused by damage to the hippocampus.

27

28 **Key words:** hydrogen sulfide, probe, fluorescence, hippocampus

29 1. Introduction

30 Hydrogen sulfide (H₂S), an colorless gas with the characteristic foul odor of
31 rotten eggs, has been considered as a toxic pollutant for more than three hundred
32 years¹. Nevertheless, recent studies indicate H₂S as the third gaseous signal molecule
33 which is almost as important as nitric oxide (NO) and carbon monoxide (CO) in
34 biological systems^{2,3,4}. H₂S may show either protective or toxic effects on cells at
35 different concentrations⁵⁻⁸. Normally, in mammalian cells, H₂S is endogenously
36 produced by enzymes such as cystathionine β-synthetase (CBS), cystathionine γ-lyase
37 (CSE), 3-mercaptopyruvate sulfurtransferase (3-MST) and cysteine lyase (CL) in
38 cysteine-related sources^{9,10}. However, accumulating evidence has confirmed that
39 abnormal H₂S concentrations are related to various diseases, including Alzheimer's
40 disease¹¹, diabetes¹² and tumor¹³, and found within many cell lines such as porcine
41 oocytes¹⁴ and MCF-7 cells¹⁵.

42 Interestingly, several studies also provide evidence supporting the excellent role
43 of H₂S in neuromodulation^{16,17}. For example, H₂S can act as a neuroprotectant, protect
44 neurons from oxidative stress, and produce potential therapeutic effects against
45 neurodegenerative disorders¹⁸⁻²⁰. Furthermore, researchers show that H₂S can inhibit
46 the apoptosis of hippocampal neurons and reduce the damage of hippocampal
47 neurons²¹⁻²⁴. Hence, more attention have been drawn on the possible role that H₂S
48 might play in neurological deficits caused by damage to the hippocampus. Thus, a
49 highly selective and sensitive analytical measurement for better understanding how
50 this gasotransmitter contributes to convoluted biological processes is directly

51 requested²⁵, which can accurately and reliably determine the biologically relevant
52 concentrations of H₂S in the nervous system.

53 Traditional analytical techniques for H₂S detection include the methylene blue
54 method, the monobromobimane method, gas chromatography and the sulfide ion
55 selective electrode method²⁶⁻²⁹. In contrast, fluorescent probes have been widely
56 applied for detecting the concentrations of H₂S in living biological systems due to
57 their high selectivity and sensitivity, short response time, non-invasive detection, and
58 real-time imaging^{30,31}. Unfortunately, the short excitation wavelength light (ca.
59 350-550 nm) limits its application in deep-tissue imaging because of the shallow
60 penetration depth. Recently, two-photon fluorescence probes, which can be excited by
61 two-photon absorption, provided an opportunity to overcome the problems originated
62 from the single-photon fluorescence technology compared with cellular imaging, the
63 organic imaging also has iconic significance owing to its more complex structures
64 and research value³²⁻³⁵. Most recently, Chen *et al.*³⁴ and Liu *et al.*³⁶ reported the
65 detection and imaging of H₂S in cardiac and liver tissues. These remind us that
66 histological-section researching is a breakthrough in *vivo* detection for H₂S.

67 In the current study, an easily synthesized benzothiazole-based fluorescent probe
68 EPS-HS was designed. Its original group has stable chemical properties and
69 fluorescence spectrum is not affected by environmental factors³⁷. Therefore, first,
70 density functional theory (DFT) calculations were performed to optimize the structure
71 of EPS-HS at the B3LYP/6-31G* level using a suite of Gaussian 09 programs^{38,39}.
72 Then the structure of the target compound was fully characterized by the standard

73 $^1\text{H-NMR}$, $^{13}\text{C-NMR}$, and high resolution mass spectrometry. Finally, the biological
74 application of EPS-HS was discussed using HT22 living cells and the hippocampus of
75 normal mice.

76

77 **2. Experimental**

78 **2.1. Synthesis of EPS-HS**

79 The synthesis process of EPS-HS is showed in Route 1. A mixture of Compound
80 **1** which was synthesized by means of the reference paper^{40,41} (0.227 g, 1.0 mmol), 2,
81 4-dinitrofluorobenzene (0.186 g, 1.0 mmol), triethylamine (0.303 g, 3.0 mmol) in 10
82 mL dry DMF (dimethyl formamide) were stirred at N_2 atmosphere, and the solution
83 was stirred at 80°C for 6 - 8 h. The reaction mixture was cooled to room temperature
84 and poured into a mixture of ice and water (100 mL) before a light yellow solid was
85 precipitated. The raw product was filtered and recrystallized from EtOAc to provide a
86 light yellow solid in 85 % yield. m.p. 128.2°C - 129.3°C . TLC (silica, hexane : DCM,
87 2:1 v/v); $R_f = 0.4$; $^1\text{H NMR}$ (400 MHz, $\text{DMSO-}d_6$), δ (ppm): 8.93 (d, $J = 2.8$ Hz, 1H),
88 8.49 (dd, $J_1 = 9.2$ Hz, $J_2 = 2.8$ Hz, 1H), 8.22-8.24 (m, 2H), 8.17 (d, $J = 8.0$ Hz, 1H),
89 8.08 (d, $J = 8.0$ Hz, 1H), 7.55-7.59 (m, 1H), 7.40-7.51 (m, 4H). $^{13}\text{C NMR}$ (100 MHz,
90 $\text{DMSO-}d_6$) δ (ppm): 121.1, 121.2, 122.4, 122.9, 123.4, 126.1, 127.2, 130.1, 130.2,
91 130.9, 135.1, 140.4, 142.6, 154.0, 154.4, 156.8, 166.5. HRMS (ESI^+): (M + H)⁺ calcd.
92 for EPS-HS ($\text{C}_{19}\text{H}_{12}\text{N}_3\text{O}_5\text{S}$) 394.0498; found 394.0489.

93 **2.2 Characterization**

94 Thin layer chromatography was performed on silica gel 60 F_{254} plates (250 μm)
95 and column chromatography was conducted over silica gel (300-400 mesh).

96 Visualization of the developed chromatogram was accomplished by a UV lamp.
97 UV-Vis absorption spectra were recorded on a Shanghai MAPADA UV-3100PC
98 UV-Visible spectrophotometer. All fluorescence measurements were recorded on a
99 Hitachi F4600 Fluorescence Spectrophotometer. The pH measurements were
100 performed on a Mettler-Toledo Delta 320 pH meter. All fluorescence imaging
101 experiments were conducted under a FV1000 confocal laser scanning microscope
102 (Olympus, Japan). All the solvents were of analytic grade. The stock solution of
103 $\text{Na}_2\text{S}\cdot 9\text{H}_2\text{O}$ ($\geq 98.0\%$) was prepared in doubly distilled water, which was freshly
104 prepared each time before use. All fluorescence measurements were carried out at
105 room temperature on a Hitachi Fluorescence Spectrophotometer F-4600. The samples
106 were excited at 285 nm with the excitation and emission slit widths set at 5.0 nm. The
107 emission spectrum was scanned from 350 nm to 560 nm at 1200 nm/min. The
108 photomultiplier voltage was set at 900 V.

109

110 **3. Results and discussion**

111 **3.1 Computational calculations**

112 DFT calculations were conducted to achieve the preferential conformation of
113 EPS-HS and its parent nucleus (Compound 1) (Figures 1A and 1B) and to investigate
114 the mechanism by which EPS-HS reacted with H_2S (Figure 1C). Results showed that
115 the photoexcitation of EPS-HS from S_0 to S_1 states mainly involved electron
116 transitions from the highest occupied molecular orbital (HOMO) to the lowest
117 occupied molecular orbital (LUMO). The HOMO of EPS-HS was mainly located at

118 the benzothiazolyl part, but the LUMO were mostly located at the nitrobenzene part.
119 It can be seen in the frontier molecular orbital diagram that the HOMO did not
120 overlap with the LUMO.

121 Based on the frontier molecular orbital theory, the computational results of
122 EPS-HS indicate that the increased electric density area is mainly within the
123 nitrobenzene part. The ether linkage becomes the target of nucleophilic reagent (H_2S).
124 There was no obvious difference as to average energy between the LUMO and the
125 HOMO.

126 **3.2 Fluorescence and absorption spectroscopy**

127 The changes in the fluorescence and absorption spectroscopy of EPS-HS ($10\ \mu\text{M}$)
128 was tested at 37°C in 20 mM PBS buffer (pH 7.4) using Na_2S ($100\ \mu\text{M}$) as a sulfide
129 source. Results showed that the maximum absorption peak of EPS-HS was shifted
130 which was similar to Compound 1 (Figure 2A). Meanwhile, a robust increase in
131 fluorescence intensity (> 40 -fold) was found with the maximum emission peak at 470
132 nm when excited at 285 nm, which was completed within 20 min (Figure 2B). These
133 data indicated that our experimental results were consistent with the frontier orbital
134 theory.

135 Next, we examined the sensitivity of EPS-HS for H_2S using various
136 concentrations of Na_2S (0 - $300\ \mu\text{M}$) (Figure 3A). Upon exposure to H_2S , the probe
137 was cleaved to release fluorophores. The fluorescence intensity was increased about 0
138 - 40 folds. Then, EPS-HS was further reacted with different concentrations of Na_2S (0
139 - $60\ \mu\text{M}$), showing a linear relationship of emission intensity versus sulfide

140 concentration in PBS buffer and fetal bovine serum (Figure S1, ESI†).

141 The fluorescence intensity of EPS-HS (10 μM) in PBS and fetal bovine serum
142 was assessed with the presence of different concentrations of Na_2S for 20 min (Figure
143 S1, Supporting Information). But, the fluorescence response in serum was lower than
144 that observed in PBS buffer, which may attribute to the fast metabolism of sulfide in
145 plasma. The fast responses and excellent linear relationship provided a real-time
146 quantitative method for detecting sulfide in biological samples. The detection limit
147 was calculated to be 108 nM in PBS butter and 154 nM in fetal bovine serum. After
148 the addition of 100 μM Na_2S buffered solution, a significant fluorescence increase
149 was observed between 0 to 45 min after mixture, and the reaction was completed at
150 37°C within 20 min (Figure 3B). Further studies indicated that the emission intensity
151 reached the peak from pH 7.0 to 9.0 (Figure S3, Supporting Information), which
152 meets the requirement of real-time detection of H_2S in the living body.

153 3.3 Selectivity of EPS-HS

154 Moreover, according to turn-on fluorescence responses, EPS-HS was found to be
155 more selective for sulfide than other biologically relevant thiols such as GSH, Cys and
156 Hcy *et al.*(Figure 4A), amino acids (Figure 4B) and other species (Figure S2,
157 Supporting Information) in PBS buffer. This may because that H_2S is a small gas
158 molecule, its $\text{pK}_{\text{a}1}$ is about 6.9, while pK_{a} value of other thiol (such as GSH, Cys) in
159 cell is higher (about 8.5). The design principle of this type probe is based on thiol pK_{a}
160 values to distinguish each other. The recognizing groups of probe EPS-HS we
161 designed is m-dinitrobenzene. The m-dinitrobenzene ether is used to protect tyrosine

162 in synthesis of peptide chain. In weak alkali conditions, using thiol as sulfur agent can
163 remove the protection group. Therefore under the physiological conditions, the probe
164 EPS-HS could detect hydrogen sulfide selectively rather than thiols like GSH and
165 Hcy.

166 **3.4 Application of EPS-HS in live-cell imaging**

167 Then, the potential ability of EPS-HS to detect H₂S was tested in HT22 cells
168 using confocal microscopy imaging (Figure 5). First of all, the cytotoxicity of
169 EPS-HS toward HT22 cells was examined by MTT assay. EPS-HS exhibited an IC₅₀
170 of 58.99 ± 1.7 μM, which demonstrated that EPS-HS was of low toxicity toward
171 cultured cell lines (Figure 5). Then, to assess the ability of EPS-HS for H₂S
172 fluorescence imaging, HT22 cells were incubated with 10 μM EPS-HS alone at 37°C
173 for 20 min (Figure 6, 1A) which is equivalent to the intracellular basal level of
174 endogenous H₂S. As expected, incrementally stronger yellowish-green fluorescence
175 was detected in HT22 cells treated with 10 μM EPS-HS and 10 μM or 100 μM Na₂S
176 (Figure 6, 2B and 3B). These results indicate that EPS-HS is readily internalized into
177 living cells and act as a fluorescent probe to detect the concentration of H₂S in living
178 cells (Figure 6C). Subsequently, cells were pretreated with ZnCl₂ (an efficient
179 eliminator of H₂S) and then incubated with EPS-HS (10 μM) for 10 min. With the
180 addition of Na₂S (100 μM) and GSH (100 μM) to the ZnCl₂-pretreated cells, no
181 fluorescence intensity increases were observed (Figure 6, 4B). The results indicated
182 that the fluorescence change of EPS-HS in the cells arises from H₂S.

183 **3.5 Application of EPS-HS in mouse hippocampus imaging**

184 We further evaluated the visualization of H₂S in KM mice hippocampal tissues
185 using EPS-HS. The mouse brains were rapidly taken and fixed in 4%
186 paraformaldehyde for 30 min. Then the tissues were embedded in ornithine
187 carbamoyltransferase (OCT), and serially sectioned at 7 μm for fluorescent detection
188 analysis (Figure 7). As shown in Figure 7A, there was no background fluorescence
189 emission for hippocampal tissue slices after incubation with PBS working fluid. When
190 the slices pretreated with Na₂S (10 μM) (Figure 7B) and Na₂S (100 μM) (Figure 7C)
191 were incubated with EPS-HS (10 μM) working fluid at 37°C for 20 min,
192 yellowish-green fluorescence signals were obviously observed. When the slices
193 pretreated with GSH (100 μM) (Figure 7D) were incubated with EPS-HS (10 μM)
194 working fluid at 37°C for 20 min, yellowish-green fluorescence signals were hardly
195 observed. These findings demonstrated that EPS-HS is capable of detecting H₂S in the
196 tissues.

197 **3.6 Detection of sulfide in mouse hippocampus**

198 Finally, EPS-HS was added to measure sulfide concentrations in mouse
199 hippocampal tissues, where the spiked Na₂S (X, X+0.2, X+0.4, X+0.6, X+0.8 μM) were
200 used as internal standard. The spiked homogenate samples were subsequently
201 precipitated by DMSO to remove proteins. To the supernatant of the spiked
202 hippocampus homogenates, EPS-HS (10 μM) was added. The mixture was incubated
203 in PBS buffer at 37°C for 20 min before analysis. We found that the average sulfide
204 concentration in fresh mouse hippocampus was 1.267 ± 0.020 μmol/g protein (Table
205 1). Overall, these findings demonstrated that EPS-HS is suitable to detect sulfide in

206 real biological samples in a rapid manner. Importantly, hydrogen sulfide is recognized
207 as a neuromodulator as well as neuroprotectant in the brain. Then, we repeated the
208 measurement with probe NAP-1⁴². The concentration of sulfide was determined to be
209 $1.242 \pm 0.047 \mu\text{mol g}^{-1}$ protein, which was consistent with the results from EPS-HS .

210 **4. Conclusions**

211 In summary, EPS-HS was designed as a benzothiazole - based H₂S fluorescent
212 probe, which shows a significant emission increase in the fast response to sulfide
213 within the biologically relevant pH range. EPS-HS produces a turn-on fluorescence
214 signal for responding H₂S. It can be applied for parallel measurement of sulfide
215 concentrations in HT22 cells and mouse hippocampus.

216 **Acknowledgements**

217 This study was financially supported by the National Natural Science Foundation
218 of China (81671069 to Y. L.), the Postdoctoral Science Foundation of China
219 (2012M521125 to L. Y) and the Open Program of Key Laboratory of Nuclear
220 Medicine, Ministry of Health and Jiangsu Key Laboratory of Molecular Nuclear
221 Medicine (KF201503).

222 **Notes and references**

- 223 1 Liu, C. *et al.* Capture and Visualization of Hydrogen Sulfide by a Fluorescent Probe.
224 *Angewandte Chemie International Edition* 50, 10327-10329 (2011).
- 225 2 Wang, X. *et al.* A near-infrared ratiometric fluorescent probe for rapid and highly sensitive
226 imaging of endogenous hydrogen sulfide in living cells. *Chemical Science* 4, 2551-2556
227 (2013).
- 228 3 Li, L., Rose, P. & Moore, P. K. Hydrogen Sulfide and Cell Signaling. *Annual Review of*
229 *Pharmacology & Toxicology* 51, 169-187 (2011).
- 230 4 Han, Y., Qin, J., Chang, X., Yang, Z. & Du, J. Hydrogen sulfide and carbon monoxide are in
231 synergy with each other in the pathogenesis of recurrent febrile seizures. *Cellular &*
232 *Molecular Neurobiology* 26, 101-107 (2006).

- 233 5 Shim, H. S. & Longo, V. A Protein Restriction-Dependent Sulfur Code for Longevity. *Cell* 160,
234 15–17 (2015).
- 235 6 Yi, L. *et al.* A Dual-Response Fluorescent Probe Reveals the H₂ O₂ -Induced H₂ S Biogenesis
236 through a Cystathionine beta-Synthase Pathway. *Chemistry (Weinheim an der Bergstrasse,*
237 *Germany)* 21, 15167-15172, doi:10.1002/chem.201502832 (2015).
- 238 7 Reiffenstein, R. J., Hulbert, W. C. & Roth, S. H. Toxicology of hydrogen sulfide. *Annual*
239 *Review of Pharmacology & Toxicology* 32, 109-134 (1992).
- 240 8 Szabo, C. *et al.* Tumor-derived hydrogen sulfide, produced by cystathionine- β -synthase,
241 stimulates bioenergetics, cell proliferation, and angiogenesis in colon cancer [Pharmacology].
242 (2013).
- 243 9 Ruth, P., Elddie, R. M. & Juan, L. G. Hydrogen sulfide and heme proteins: knowledge and
244 mysteries. *Antioxidants & Redox Signaling* 15, 393-404 (2011).
- 245 10 Shibuya, N. *et al.* 3-Mercaptopyruvate Sulfurtransferase Produces Hydrogen Sulfide and
246 Bound Sulfane Sulfur in the Brain | Abstract. *Mary Ann Liebert Inc Huguenot Street Floor*
247 *New Rochelle Ny Usa.*
- 248 11 Eto, K., Asada, T., Arima, K., Makifuchi, T. & Kimura, H. Brain hydrogen sulfide is severely
249 decreased in Alzheimer's disease. *Biochemical & Biophysical Research*
250 *Communications* 293, 1485–1488 (2002).
- 251 12 Wu, L. *et al.* Pancreatic islet overproduction of H₂S and suppressed insulin release in Zucker
252 diabetic rats. *Laboratory Investigation* 89, 59-67 (2008).
- 253 13 Emanuela, P. *et al.* Hydrogen sulfide promotes calcium signals and migration in tumor-derived
254 endothelial cells. *Free Radical Biology & Medicine* 51, 1765-1773 (2011).
- 255 14 Nevoral, J. *et al.* Endogenously produced hydrogen sulfide is involved in porcine oocyte
256 maturation in vitro. *Nitric Oxide* 51, 24-35 (2015).
- 257 15 Li, H. D. *et al.* A fluorescent probe for H₂S in vivo with fast response and high sensitivity.
258 *Chemical Communications* 51, 16225-16228 (2015).
- 259 16 Lu, M. *et al.* Hydrogen sulfide regulates intracellular pH in rat primary cultured glia cells.
260 *Neuroscience Research* 66, 92-98 (2010).
- 261 17 ZHOU, Cheng-fang, TANG & Xiao-qing. Hydrogen sulfide and nervous system regulation.
262 *Chinese Medical Journal* 124, 3576-3582 (2011).
- 263 18 Schreier, S. M. *et al.* Hydrogen Sulfide Scavenges the Cytotoxic Lipid Oxidation Product
264 4-HNE. *Neurotoxicity Research* 17, 249-256 (2010).
- 265 19 Tiong, C. X., Lu, M. & Bian, J. S. Protective effect of hydrogen sulphide against
266 6-OHDA-induced cell injury in SH-SY5Y cells involves PKC/PI3K/Akt pathway. *British*
267 *Journal of Pharmacology* 168, 2011–2012 (2013).
- 268 20 Kida, K. *et al.* Inhaled hydrogen sulfide prevents neurodegeneration and movement disorder
269 in a mouse model of Parkinson's disease. *British Journal of Industrial Relations* 50, 590-592
270 (2011).
- 271 21 Lefer, D. J. A new gaseous signaling molecule emerges: cardioprotective role of hydrogen
272 sulfide. *Proceedings of the National Academy of Sciences* 104, 17907-17908 (2007).
- 273 22 Zanardo, R. C. *et al.* Hydrogen sulfide is an endogenous modulator of leukocyte-mediated
274 inflammation. *Faseb Journal Official Publication of the Federation of American Societies for*
275 *Experimental Biology* 20, 2118-2120 (2006).
- 276 23 JW, E. *et al.* Hydrogen sulfide attenuates myocardial ischemia-reperfusion injury by

- 277 preservation of mitochondrial function. *Proceedings of the National Academy of Sciences of*
278 *the United States of America* 104, 15560-15565 (2007).
- 279 24 Y, K., Y, K., H, K. & I, N. L-cysteine inhibits insulin release from the pancreatic beta-cell:
280 possible involvement of metabolic production of hydrogen sulfide, a novel gasotransmitter.
281 *Diabetes* 55, 1391-1397 (2006).
- 282 25 Chem., A. Visualization of In Vivo Hydrogen Sulfide Production by a Novel Bioluminescence
283 Probe in Cancer Cells and Nude Mice. *Analytical Chemistry* (2015).
- 284 26 Ishigami, M. *et al.* A source of hydrogen sulfide and a mechanism of its release in the brain.
285 *Antioxidants & Redox Signaling* 11, 205-214 (2009).
- 286 27 Doeller, J. E. *et al.* Polarographic measurement of hydrogen sulfide production and
287 consumption by mammalian tissues. *Analytical Biochemistry* 341, 40-51 (2005).
- 288 28 Lawrence, N. S. *et al.* The Electrochemical Analog of the Methylene Blue Reaction: A Novel
289 Amperometric Approach to the Detection of Hydrogen Sulfide. *Electroanalysis* 12, 1453-1460
290 (2000).
- 291 29 Zhou, X., Lee, S., Xu, Z. & Yoon, J. Recent Progress on the Development of Chemosensors
292 for Gases. *Chemical Reviews* 115, 7944-8000 (2015).
- 293 30 Zhang, H. *et al.* An iminocoumarin benzothiazole-based fluorescent probe for imaging
294 hydrogen sulfide in living cells. *Talanta* 135, 2310-2313 (2015).
- 295 31 Zhang, C. *et al.* A Redox-Nucleophilic Dual-Reactable Probe for Highly Selective and
296 Sensitive Detection of H₂S: Synthesis, Spectra and Bioimaging. *Scientific Reports* 6 (2016).
- 297 32 Sajal Kumar, D., Su, L. C., Young, Y. S., Hee, H. J. & Bong Rae, C. A small molecule
298 two-photon probe for hydrogen sulfide in live tissues. *Cheminform* 48, 8395-8397 (2012).
- 299 33 Sung Keun, B. *et al.* A ratiometric two-photon fluorescent probe reveals reduction in
300 mitochondrial H₂S production in Parkinson's disease gene knockout astrocytes. *Journal of the*
301 *American Chemical Society* 135, 9915-9923 (2013).
- 302 34 Chen, B. *et al.* Fluorescent probe for highly selective and sensitive detection of hydrogen
303 sulfide in living cells and cardiac tissues. *Analyst* 138, 946-951 (2013).
- 304 35 Gryko, D. T. *et al.* Dipolar Dyes with Pyrrolo[2,3 - b]quinoxaline Skeleton Containing a
305 Cyano Group and a Bridged Tertiary Amino Group - Synthesis, Solvatochromism
306 and Bioimaging. *Chemistry An Asian Journal* 11 (2016).
- 307 36 Liu, Y., Meng, F., He, L., Liu, K. & Lin, W. A dual-site two-photon fluorescent probe for
308 visualizing lysosomes and tracking lysosomal hydrogen sulfide with two different sets of
309 fluorescence signals in the living cells and mouse liver tissues. *Chemical Communications* 52,
310 7016-7019 (2016).
- 311 37 Riswan Ahamed, M. A., Azarudeen, R. S. & Kani, N. M. Antimicrobial Applications of
312 Transition Metal Complexes of Benzothiazole Based Terpolymer: Synthesis, Characterization,
313 and Effect on Bacterial and Fungal Strains. *Bioinorganic Chemistry & Applications* 2014,
314 764085-764085 (2014).
- 315 38 Frisch, M. *et al.* Gaussian 09, revision A. 02; Gaussian, Inc. Wallingford, CT 19, 227-238
316 (2009).
- 317 39 Frisch, M. *et al.* (Gaussian, Inc. Wallingford, CT, 2009).
- 318 40 Liu, S. D., Zhang, L. W. & Liu, X. A highly sensitive and selective fluorescent probe for Fe³⁺
319 based on 2-(2-hydroxyphenyl)benzothiazole. *New Journal of Chemistry* 37, 821-826 (2013).
- 320 41 Pratap, U. R., Mali, J. R., Jawale, D. V. & Mane, R. A. Bakers' yeast catalyzed synthesis of

321 benzothiazoles in an organic medium. *Tetrahedron Letters* 50, 1352-1354 (2009).
322 42 Ling, Z. *et al.* A colorimetric and ratiometric fluorescent probe for the imaging of endogenous
323 hydrogen sulphide in living cells and sulphide determination in mouse hippocampus. *Organic*
324 & *Biomolecular Chemistry* 12, 5115-5125 (2014).

325

ACCEPTED MANUSCRIPT

326

Article---Figure Legends

327 **Figure 1. Optimized, low-energy conformations of the benzothiazole rings using DFT**

328 **(B3LYP/6-31G*) calculations:** (A) Compound 1. (B) EPS-HS. (C) the structure of EPS-HS on
329 the HOMO and LUMO.

330 **Route 1.** The synthetic route of EPS-HS.

331 **Figure 2.** Fluorescence spectra (A) and absorption spectra (B) of EPS-HS (10 μM), Compound 1
332 (10 μM) and EPS-HS (10 μM) + Na_2S (100 μM) in PBS buffer (20 mM, pH = 7.4, 5% DMSO).

333 **Figure 3.** Fluorescence spectra of EPS-HS (10 μM) in PBS buffer (20 mM, pH 7.4, 5% DMSO) at
334 37°C for 20 min. Excitation: 285 nm, emission: 350 - 560 nm. (A) Incubated with different
335 concentrations of Na_2S (0, 1.0, 2.0, 5.0, 10, 20, 30, 40, 50, 60, 80, 100, 150, 200 and 300 μM) for
336 20 min. (B) Incubated with 100 μM Na_2S after 0, 4, 6, 8, 10, 12, 14, 16, 18, 20, 25, 30, 45 min.
337 Excitation: 285 nm, emission: 350 - 560 nm. Data are presented as the mean \pm SD (n = 3).

338 **Figure 4.** Fluorescence responses of EPS-HS (10 μM) towards Na_2S (100 μM) and various
339 biothiols after 20 min of treatment. (A) (1) Na_2S (0 μM); (2) Na_2S (100 μM); (3) Hcy (100 μM);
340 (4) GSH (100 μM); (5) Cys (100 μM); (6) Hcy (1 mM); (7) GSH (1 mM); (8) Cys (1 mM); (9)
341 Na_2S (100 μM)+Hcy (100 μM); (10) Na_2S (100 μM) +Hcy (1 mM); (11) Na_2S (100 μM) + GSH
342 (100 μM); (12) Na_2S (100 μM) + GSH (1 mM); (13) Na_2S (100 μM) + Cys (100 μM); and (14)
343 Na_2S (100 μM) + Cys (1 mM). (B) Fluorescence responses of EPS-HS (10 μM) towards Na_2S
344 (100 μM) and amino acids. Data are presented as the mean \pm SD (n = 3).

345 **Figure 5.** (A) The inhibitory effect of EPS-HS on the cell growth of HT22 cells after treatment for
346 24 h. (B) The viability of HT22 cells after exposure to EPS-HS (10.0 μM) for different times. Data
347 are presented as the mean \pm SD (n = 3).

348 **Figure 6. Confocal fluorescence images in living cells.** HT22 cells were incubated with EPS-HS
349 alone (10 μM) for 20 min (1A and 1B). The cells were exposed to EPS-HS (10 μM) followed by
350 Na_2S (10 μM) at 37°C for 20 min (2A). The cells were exposed to EPS-HS (10 μM) followed by
351 Na_2S (100 μM) at 37°C for 20 min (3A). Cells were pretreated with 1 mM ZnCl_2 for 10 min, then
352 incubated with EPS-HS (10 μM) for 10 min and then incubated with Na_2S (100 μM) and GSH (100
353 μM) at 37°C for 20 min (4A); Overlay of the bright field image and the green channel (2B, 3B and
354 4B). Fluorescence intensity per one cell. Fluorescence images were acquired by confocal
355 microscopy (C). Scale bars = 10 μm . Data are presented as the mean \pm SD (n = 3).

356 **Figure 7. *In situ* visualization of hippocampal tissues of the brains with EPS-HS.** An image of
357 frozen mouse hippocampal slices incubated with PBS working fluid (A); an image of frozen
358 mouse hippocampal slices incubated with EPS-HS (10 μM) working fluid after pretreatment with
359 Na_2S (10 μM) (B) and Na_2S (100 μM) (C) at 37°C for 20 min; Slices pretreated with GSH (100
360 μM) were incubated with EPS-HS (10 μM) working fluid at 37°C for 20 min (D). Scale bars = 20
361 μm . The mean fluorescence intensity was obtained with 6-8 slices from different mice.

362 **Table 1.** Measurement of sulfide concentrations in fresh mouse hippocampus tissues.

363

364

Electronic Supplementary Information for

365

A benzothiazole-based fluorescent probe for selective

366

detection of H₂S in living cells and mouse hippocampal

367

tissues

368

369 Yi Liu,^{*#a} Yan Ding,^{*a} Jie Huang,^a Xiaofei Zhang,^a Tongyong Fang,^a Yuyun Zhang,^a370 Xian Zheng,^a and Xia Yang^a

371

372

373 ^a Jiangsu Key Laboratory of New Drug Research and Clinical Pharmacy, School of

374 Pharmacy, Xuzhou Medical University Xuzhou, 221004 Jiangsu, China.

375 [#] Fax: +86-0516-83262136, E-mail: cbpeluyinew@163.com.

376

- 377 **1. General information**
- 378 **2. Preparation of the test solutions**
- 379 **3. Routes and characterization of Compound 1**
- 380 **4. Evidence of mechanism detection**
- 381 **5. UV-Vis absorption spectrogram**
- 382 **6. Determination of the detection limit**
- 383 **7. MTT Assay**
- 384 **8. Fluorescence imaging in living HT22 cells**
- 385 **9. In situ fluorescent detection of H₂S in the hippocampal tissues of the brains**
- 386 **Figure S1. EPS-HS probe incubated with different concentrations of Na₂S**
- 387 **Figure S2. Selectivity of EPS-HS towards other species**
- 388 **Figure S3. Fluorescence spectra of EPS-HS with the presence of Na₂S in buffer**
- 389 **solutions at different pH values**
- 390 **Figure S4. ¹H NMR spectrum of Compound 1**
- 391 **Figure S5. HR-MS spectrum of EPS-HS**
- 392 **Figure S6. ¹H NMR spectrum of EPS-HS**
- 393 **Figure S7. ¹³C NMR spectrum of EPS-HS**

394 1. Preparation of the test solutions

395 1.1 EPS-HS stock solution

396 EPS-HS (3.93 mg, 1 mmol) was dissolved into DMSO (10 mL) to get 1.0 mM
397 stock solution for general use.

398 1.2 Na₂S stock solution

399 5 mg EDTA was dissolved in 10 mL DI H₂O in a 25 mL volumetric flask. The
400 solution was purged vigorously with nitrogen gas for 15 min. Then 48 mg sodium
401 sulfide (Na₂S·9H₂O) was dissolved in the solution under nitrogen gas. The resulting
402 solution was 20 mM Na₂S, which was then diluted to 1.0 - 2.0 mM stock solution for
403 general use.

404 405 2. Route and characterization of Compound 1

406 2-Aminothiophenol (0.625 g, 5 mmol) and 4-hydroxybenzaldehyde (0.611 g, 5
407 mmol) which was dissolved in 20 mL dry ethanol were added to a 250 mL
408 eggplant-shape flask equipped with a magnetic stirrer. Aq 37% HCl (15.0 mmol) and
409 aq 30% H₂O₂ (30 mmol) were added and the mixture was stirred for 1.5 h at room
410 temperature. A light yellow crystal was got by filtration. Then, the crude product was
411 purified by flash chromatography on silica gel obtaining at a yield of 92%. m.p.
412 188°C - 189.2°C. TLC (silica, hexane : EtOAc, 3:1 v/v): R_f = 0.3.

413 ¹H NMR (400 MHz, DMSO-*d*₆) δ (ppm): 12.54 (s, 1H), 8.02 (d, *J* = 8.0 Hz, 1H),
414 7.93 (d, *J* = 8.0 Hz, 1H), 7.72 (dd, *J*₁ = 8.0 Hz, *J*₂ = 1.6 Hz, 1H), 7.51-7.55 (m, 1H),
415 7.39-7.46 (m, 2H), 7.13-7.15 (m, 1H), 6.97-7.01 (m, 1H). ESI-MS (m/z): 228.1 [M +

416 $\text{H}]^+$, calcd. for $\text{C}_{13}\text{H}_9\text{NOS} = 227.04$.

417

418 **3. Evidence of mechanism detection**

419 EPS-HS (78.6 mg, 0.2 mmol) was dissolved in DMSO (15 mL), followed by the
420 addition of $\text{Na}_2\text{S} \cdot 9\text{H}_2\text{O}$ (240 mg, 1.0 mmol) in PBS buffer (15 mL, 20 mM, pH = 7.4).
421 The resultant mixture was stirred at room temperature for 3 h. Subsequently, EtOAc
422 (3×10 mL) was added into the solution for extraction. The thiolysis product was
423 characterized by HRMS and ^1H NMR.

424

425 **4. UV-Vis absorption spectrogram**

426 Na_2S is widely recognized as H_2S donor. EPS-HS (10.0 μM) was dissolved in
427 DMSO, which was then diluted in PBS buffer (2:3, v/v, 20 mM, pH 7.4) with 5%
428 DMSO. Before the addition of Na_2S , EPS-HS (10 μM) displayed an absorption peak
429 at 285 nm. After incubated with Na_2S (100 μM) in doubly distilled water for 20 min, a
430 new absorption peak was presented at 386 nm.

431

432 **5. Determination of the detection limit**

433 The detection limit was calculated based on the method reported in previous
434 literature. The fluorescence emission spectrum of EPS-HS without Na_2S was
435 measured by 10 times and the standard deviation of blank measurement was obtained.
436 Then, the solution was treated with Na_2S at concentrations from 0 to 60 μM . A linear
437 regression curve was then achieved. The detection limit was calculated with the
438 following equation: Detection limit = $3\sigma/k$, where σ is the standard deviation of blank

439 measurements, and k is the slope between the fluorescence intensity ratios and Na_2S
440 concentrations. The detection limit was 108 nM in PBS buffer and 154 nM in fetal
441 bovine serum, respectively.

442

443 **6. MTT assay**

444 The effect of EPS-HS on cell growth was measured using a colorimetric MTT
445 assay kit (Sigma-Aldrich). HT22 cells were seeded in 96-well plates at a density of
446 50,000 cells/well and then maintained in DMEM medium with 10% fetal bovine
447 serum/penicillin/streptomycin in a 5 % CO_2 atmosphere at 37°C. The cells were
448 incubated with different concentrations of EPS-HS for 24 h, respectively. HT22 cells
449 in culture medium without EPS-HS were used as control. Then, 20 μL of MTT dye
450 (3-[4, 5-dimethylthiazol-2-yl]- 2, 5-diphenyl tetrazolium bromide, 5 mg/mL in
451 phosphate buffered saline), was added to each well, and the plates were incubated at
452 37 °C for 4 h. Then, the remaining MTT solution was removed, and 150 μL of DMSO
453 was added to each well to dissolve the formazan crystals. The plate was shaken for 10
454 min and the absorbance was measured at 570 nm on a microplate reader (ELX808IU,
455 Bio-tek Instruments Inc, USA). Each sample was performed in triplicate, and the
456 entire experiment was repeated three times. Calculation of IC_{50} values was done
457 according to Huber and Koella¹.

458

459 **7. Fluorescence imaging in living HT22 cells**

460 HT22 cells were seeded in a 6-well plate in DMEM supplemented with 10 %

461 fetal bovine serum in an environment of 5 % CO₂ at 37°C for 24 h. For a control
462 experiment, HT22 cells were incubated with EPS-HS (10 µM) at 37°C for 60 min.
463 After washing with PBS three times to remove the remaining dyes, the cells were then
464 incubated with Na₂S (10 µM) or Na₂S (100 µM) for another 20 min. The fluorescence
465 imaging was carried out after washing with PBS buffer for three times.

466

467 **8. In *situ* fluorescent detection of H₂S in the hippocampal tissues of** 468 **the brains**

469 The mouse brains were rapidly taken and fixed in 4 % paraformaldehyde. Then
470 the tissues were embedded in ornithine carbamoyltransferase (OCT), and serially
471 sectioned at 7 µm using a Leica CM1950 cryostat (Leica Microsystems, Wetzlar,
472 Germany) for fluorescence detection. After dried for 1 h, the frozen sections were
473 washed for 3 times with 10 mM PBS for 3 min. The slices treated with Na₂S (100 µM)
474 were incubated with EPS-HS working fluid (10 µM) at 37°C for 20 min and
475 subsequently rinsed in PBS for 3 times for 3 min. The slices were mounted with 50 %
476 buffered glycerol before observation under a fluorescence microscope in time. The
477 mean fluorescence intensity was obtained using 6 - 8 slices from different mice.

478

Figure Legends

479 **Figure S1.** EPS-HS probe (10 μM) incubated with 0, 1.0, 2.0, 5.0, 10, 20, 30, 40, 50, and 60 μM
480 Na_2S at 37°C for 20 min in PBS buffer (A) and fetal bovine serum (B) (5 % DMSO). The insert: A
481 graph of the fluorescence intensity trend of EPS-HS (10 μM) with the presence of different
482 concentrations of Na_2S for 20 min in PBS buffer (20 mM, pH = 7.4, 5 % DMSO) and fetal bovine
483 serum (5 % DMSO), respectively. Data are presented as the mean \pm SD (n = 3).

484 **Figure S2.** (A) Fluorescence spectra of EPS-HS (10 μM) with Na_2S (100 μM) and biologically
485 relevant species in 20 mM PBS (pH 7.4) at 37°C for 20 min. (B) Fluorescence responses of
486 EPS-HS (10 μM) towards Na_2S (100 μM) and biologically relevant species. (1) Blank, (2) Na_2S ,
487 (3) H_2O_2 , (4) OCl^- , (5) O^{2-} , (6) $-\text{OH}$, (7) $^t\text{BuOOH}$, (8) NO_2^- , (9) NO , (10) S-nitroso glutathione, (11)
488 KCl , (12) ZnSO_4 , (13) CaCl_2 , (14) MgCl_2 , (15) FeCl_3 , (16) NaCl , (17) NaH_2PO_4 , (18) NADH , (19)
489 Glucose, (20) $\text{S}_2\text{O}_3^{2-}$, (21) $\text{S}_2\text{O}_5^{2-}$, (22) $\text{S}_2\text{O}_4^{2-}$, (23) SO_3^{2-} , (24) SO_4^{2-} , and (25) SCN^- .

490 **Figure S3.** (A) Fluorescence spectra of EPS-HS (10 μM) with Na_2S (100 μM) in buffer solutions
491 at different pH values (20 mM, pH 5.8, 6.2, 6.6, 7.0, 7.4, 7.8, 8.2, 8.6, and 9.0, 5 % DMSO) at
492 37°C for 20 min. (B) Fluorescence responses of EPS-HS (10 μM) with Na_2S (100 μM) in buffer
493 solutions at different pH values (20 mM, pH 5.8, 6.2, 6.6, 7.0, 7.4, 7.8, 8.2, 8.6, and 9.0, 5 %
494 DMSO) at 37°C for 20 min.

495 **Figure S4.** ^1H NMR spectrum of Compound 1.

496 **Figure S5.** HR-MS spectrum of EPS-HS.

497 **Figure S6.** ^1H NMR spectrum of EPS-HS.

498 **Figure S7.** ^{13}C NMR spectrum of EPS-HS.

499

500 1 Huber, W. & Koella, J. C. A comparison of three methods of estimating EC 50 in studies of
501 drug resistance of malaria parasites. *Acta Tropica* **55**, 257-261 (1993).
502

ACCEPTED MANUSCRIPT

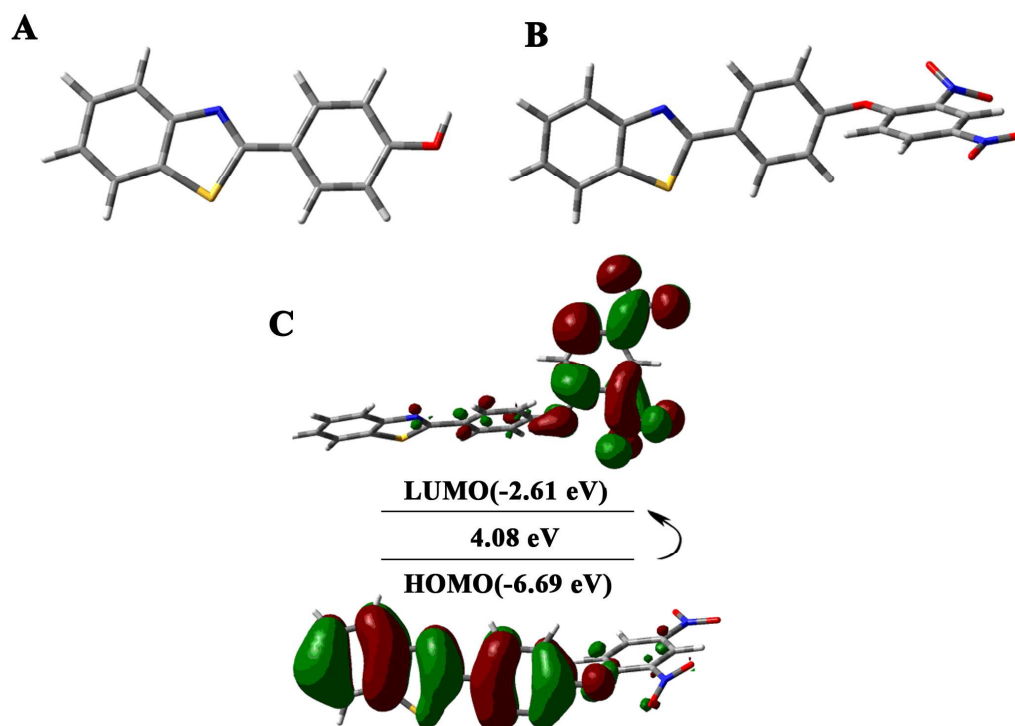
Table 1.

Sample	H ₂ S ^a (μ mol g ⁻¹ protein)	H ₂ S ^b (μ mol g ⁻¹ protein)
1	1.275	1.201
2	1.245	1.231
3	1.282	1.294
Mean \pm SD	1.267 \pm 0.020	1.242 \pm 0.047

^a Measurement of H₂S concentrations in mouse hippocampus with EPS-HS; ^b Measurement of H₂S concentrations in mouse hippocampus with NAP-1; data are presented as mean \pm SD.

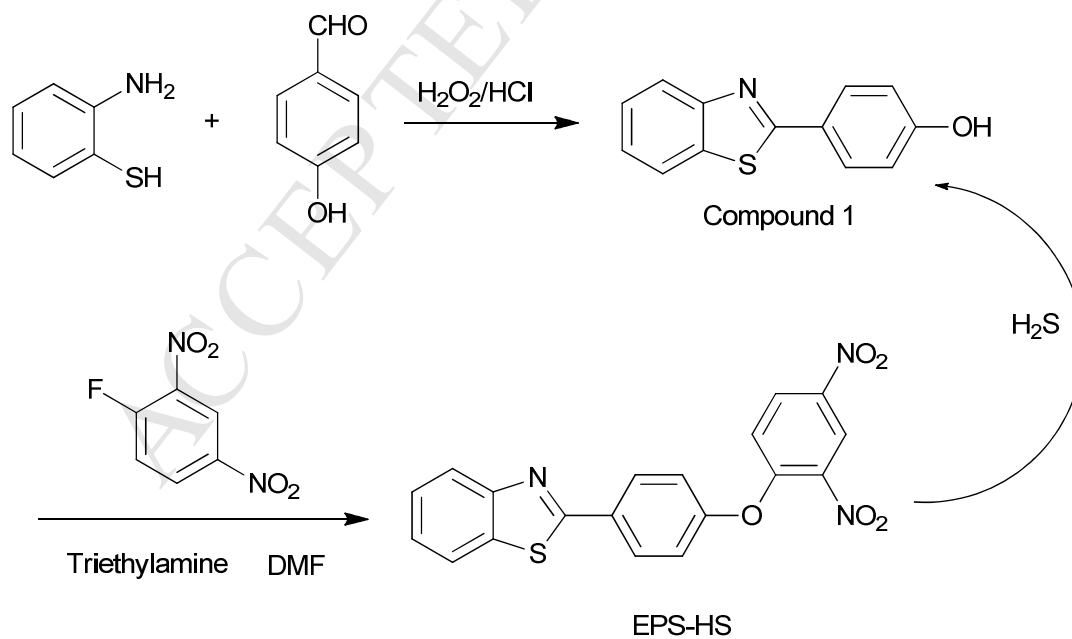
1

Figures

2 **Figure 1.**

3

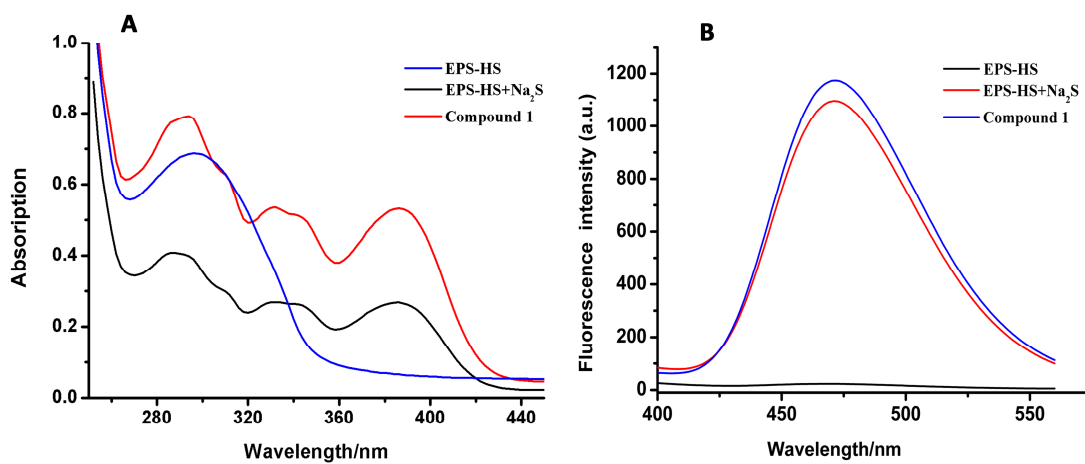
4

5 **Route 1.**

6

7

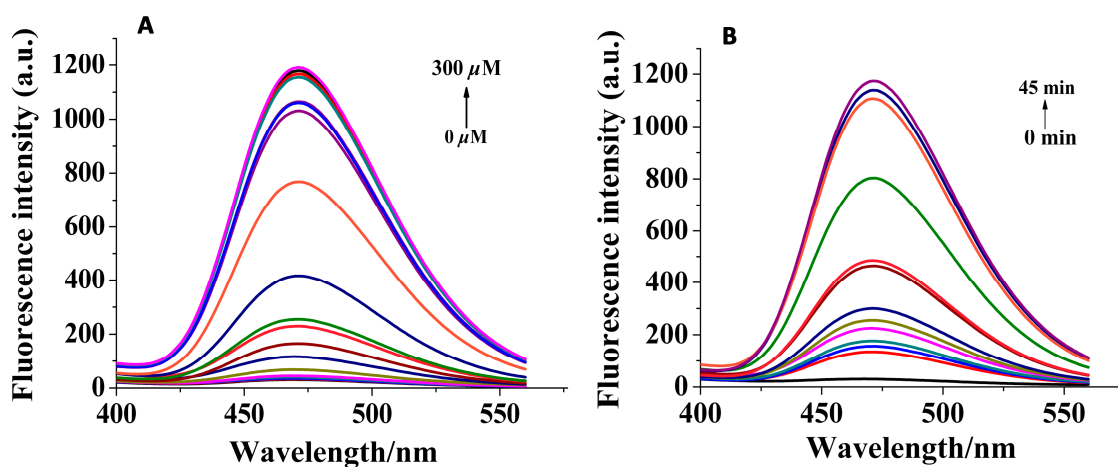
8

9 **Figure 2.**

10

11

12

13 **Figure 3.**

14

15

16

17

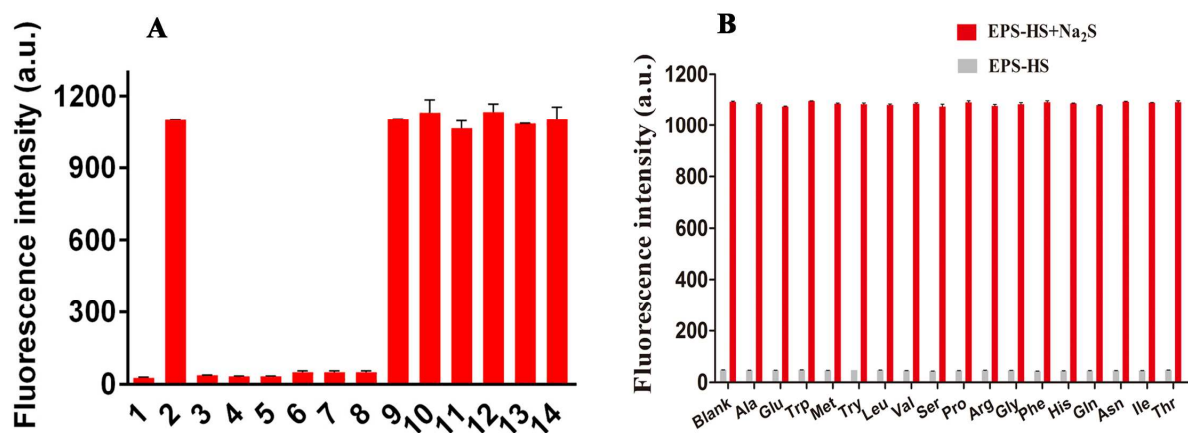
18

19

20

21

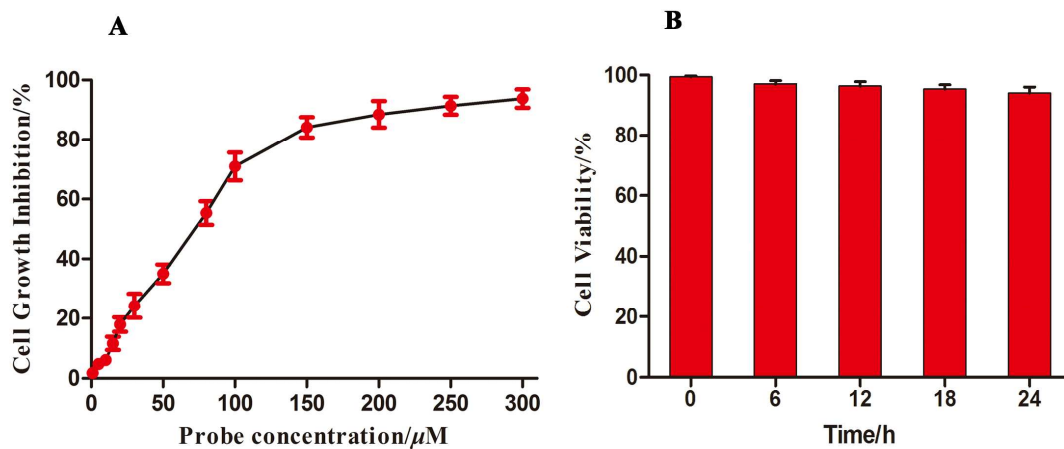
22

23 **Figure 4.**

24

25

26

27 **Figure 5.**

28

29

30

31

32

33

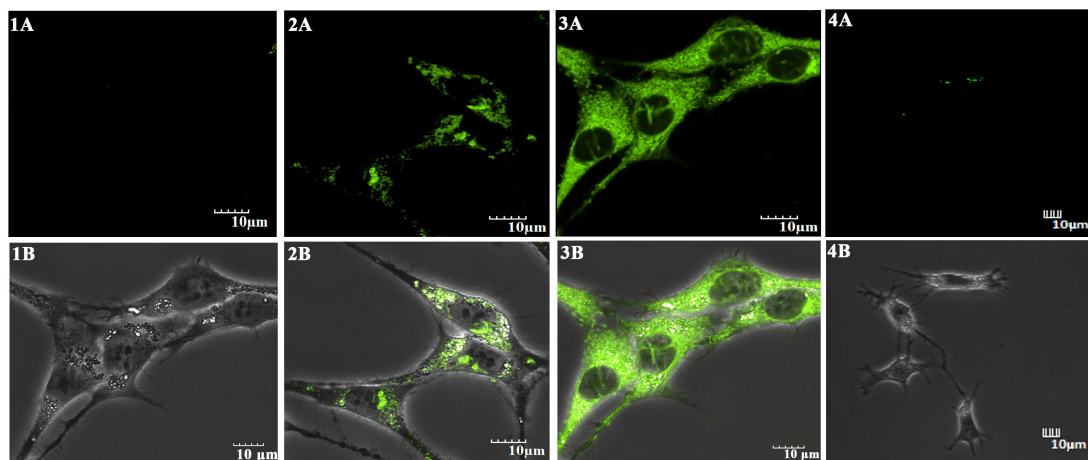
34

35

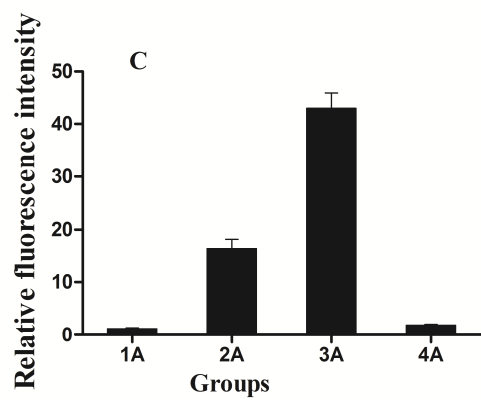
36

37 **Figure 6.**

38



39



40

41

42

43

44

45

46

47

48

49

50

51

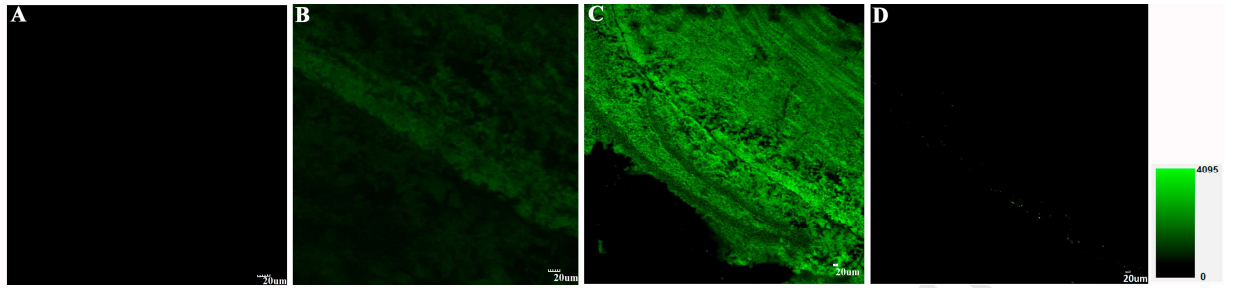
52

53

54 **Figure 7.**

55

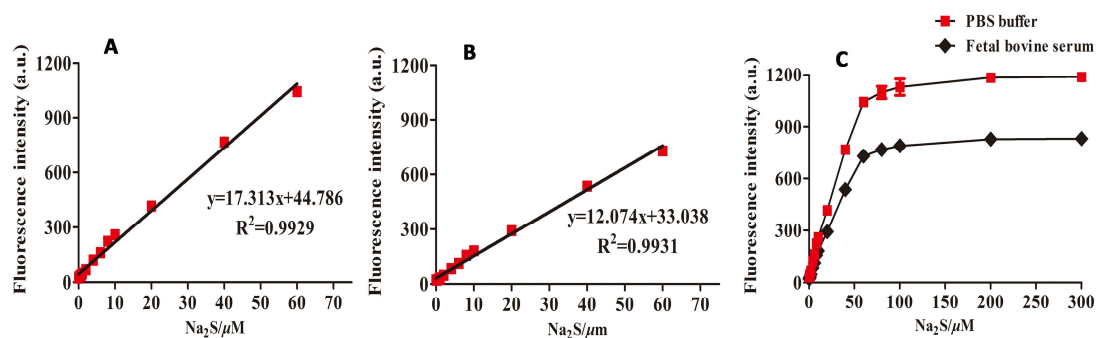
56



ESI-Figures

57

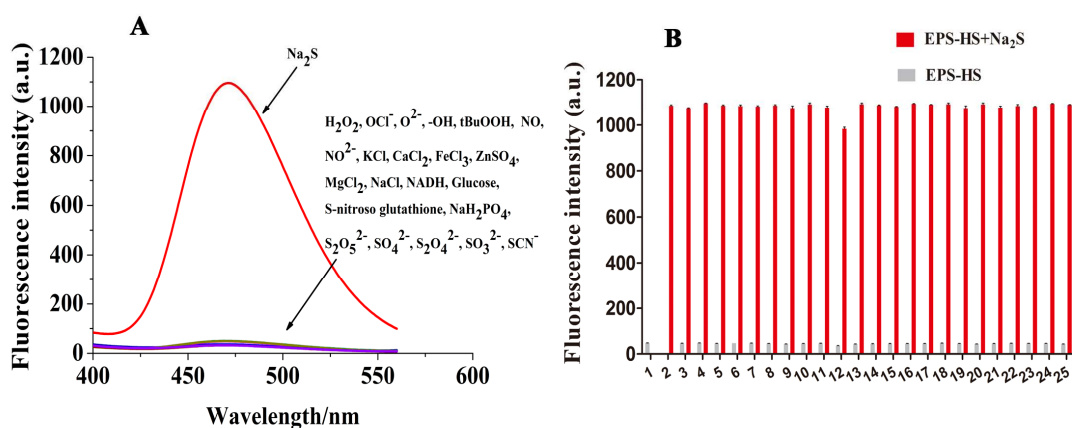
58 Figure S1.



59

60

61 Figure S2.

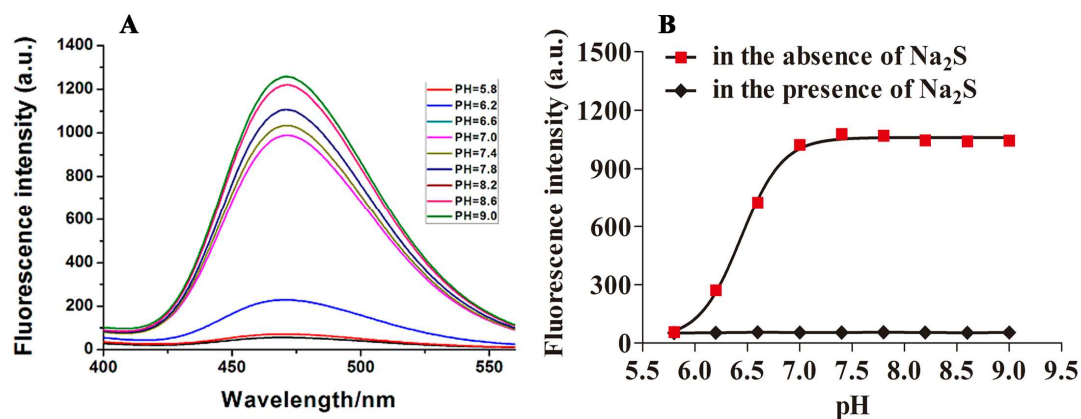


62

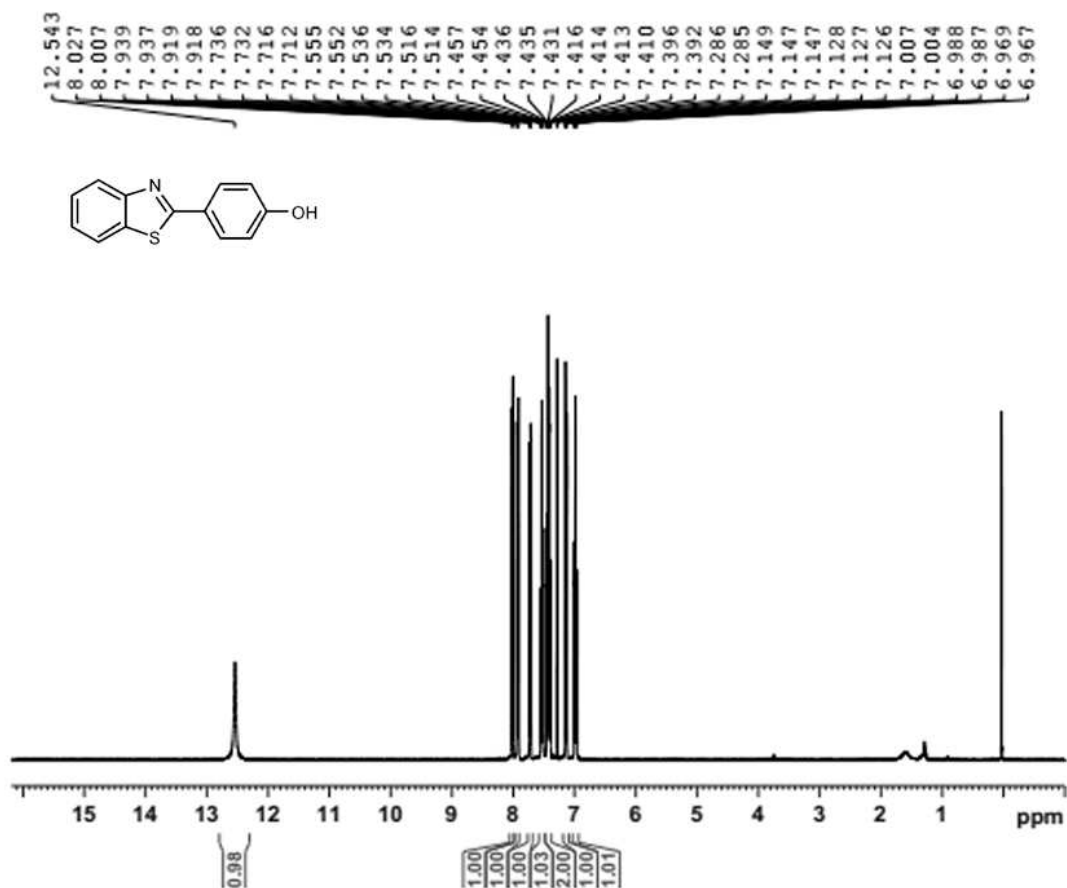
63

64

65 Figure S3.



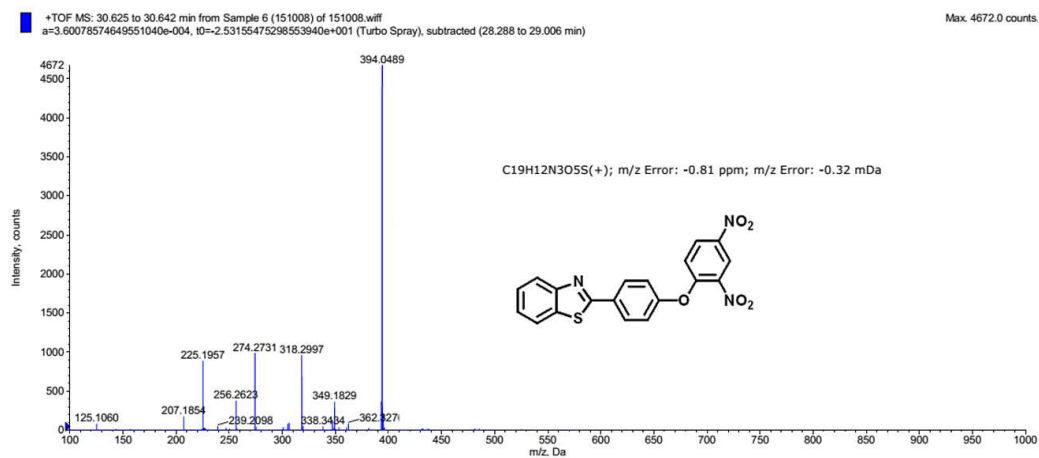
66

67 **Figure S4.**

68

69

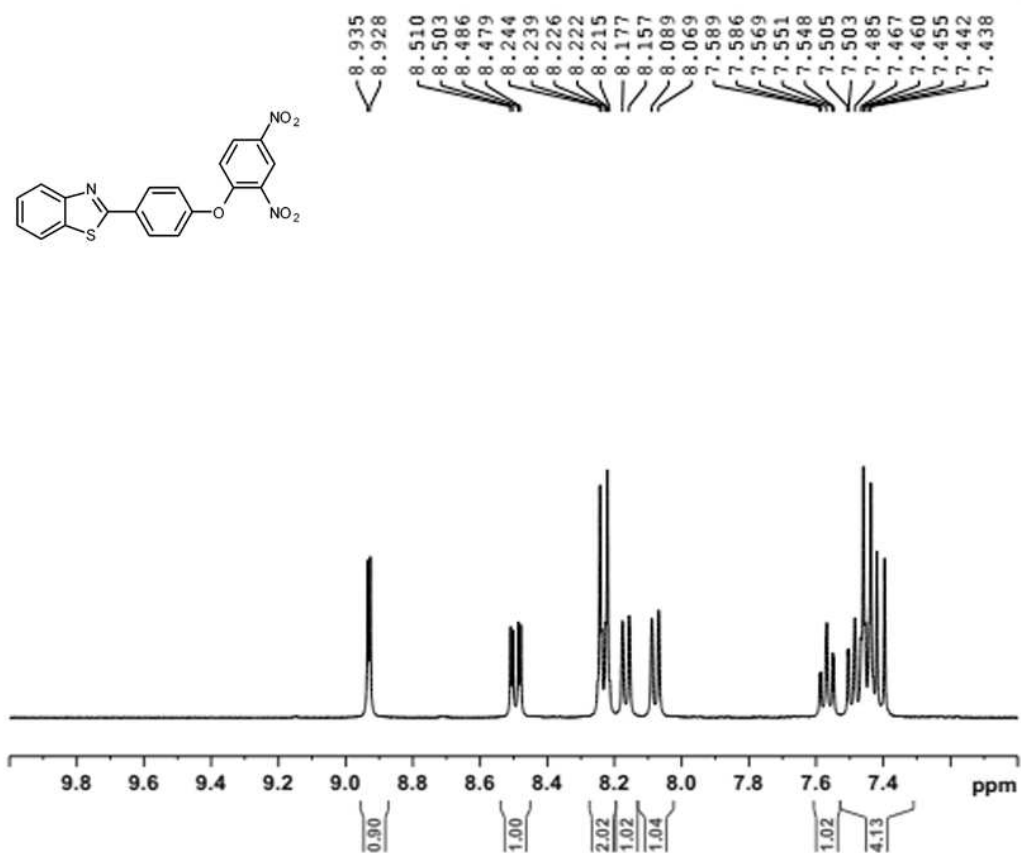
70

71 **Figure S5.**

72

73

74

75 **Figure S6.**

76

77

78

79

80

81

82

83

84

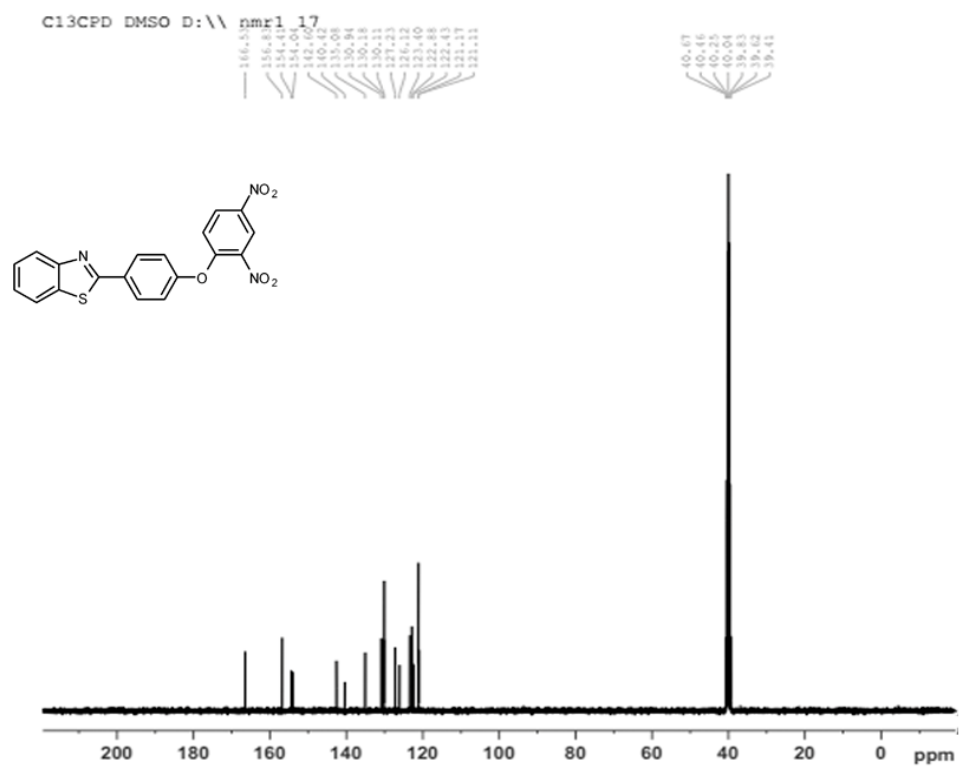
85

86

87

88

89

90 **Figure S7.**

91

Research highlights

1. We designed and synthesized a benzothiazole-based fluorescent probe EPS-HS for selective detection of H₂S.
2. The probe EPS-HS showed good cell permeability and H₂S could be detected within the cells
3. *In situ* visualization of H₂S was performed on the hippocampal slices of normal mice with probe EPS-HS.
4. The probe will be applied for better treatment of neurological deficits caused by damage to the hippocampus.